Published in final edited form as:

Eur J Nucl Med Mol Imaging. 2017 August ; 44(9): 1501–1510. doi:10.1007/s00259-017-3676-6.

Microsurgery Guided by Sequential Preoperative Lymphography using ^{68}Ga-NEB PET and MRI in Patients with Lower-limb Lymphedema

Xiao Long[1,*], **Jingjing Zhang**[2,4,*], **Daming Zhang**[3,*], **Chao Gao**[1], **Chongwei Chi**[5], **Elan Yang**[1], **Huadan Xue**[3], **Lixin Lang**[4], **Gang Niu**[4], **Zhaohui Zhu**[2,#], **Fang Li**[2], and **Xiaoyuan Chen**[4,#]

[1]Department of Plastic Surgery, Peking Union Medical College Hospital, Chinese Academy of Medical Sciences and Peking Union Medical College, Beijing 100730, China

[2]Department of Nuclear Medicine, Peking Union Medical College Hospital, Chinese Academy of Medical Sciences and Peking Union Medical College, Beijing 100730, China

[3]Department of Radiology, Peking Union Medical College Hospital, Chinese Academy of Medical Sciences and Peking Union Medical College, Beijing 100730, China

[4]Laboratory of Molecular Imaging and Nanomedicine (LOMIN), National Institute of Biomedical Imaging and Bioengineering (NIBIB), National Institutes of Health (NIH), Bethesda, Maryland, 20892, USA

[5]Key Laboratory of Molecular Imaging of Chinese Academy of Sciences, Institute of Automation, Chinese Academy of Sciences, Beijing 100190, China

Abstract

Objective—The popularity of contemporary microsurgical techniques in treatment of lower-limb lymphedema calls for better visualization of the lymphatic system, both preoperatively and intraoperatively. The aim of this prospective study was to investigate the feasibility of a novel combination of ^{68}Ga-NEB PET with MR lymphography (MRL) in evaluating lymphedema and guiding surgical intervention.

Methods—A total of 11 patients (F 9, M 2, age range 29–69 y) with lower limb lymphedema classified into stage I to III were recruited. PET acquisition was performed at 30, 60, and 90 min after subcutaneous injection of the albumin-binding radiotracer ^{68}Ga-NEB into the bilateral first web spaces of the feet. All the patients were also subjected to ^{99m}Tc-sulfur colloid (SC) lymphoscintigraphy for comparison. Gd-DTPA enhanced MRI was performed using sequences specialized for lymphatic vessel scans. All the patients underwent surgical interventions within a

[#]Corresponding authors: Zhaohui Zhu (zhuzhh@pumch.cn), Xiaoyuan Chen (shawn.chen@nih.gov).
[*]Xiao Long, Jingjing Zhang and Daming Zhang contributed equally to this work

Conflicts of interest:
None declared.

Statement of human rights
All procedures performed in studies involving human participants were in accordance with the ethical standards of the institutional and/or national research committee and with the 1964 Helsinki declaration and its later amendments or comparable ethical standards.

Informed consent
Informed consent was obtained from all individual participants included in the study.

week. The surgical approach includes the use of linear marker for edema localization and ICG lymphography with near-infrared surgical navigation system intraoperatively.

Results—Lymph transport in lymphatic channels was clearly observed by visualization of ^{68}Ga-NEB activity in the lymphatic vessels and within lymph nodes for all the 11 patients as well as the visualization of edema section plane with dermal backflow (DB), abnormally increased and disconnected uptake along the lymphatic channels. Preoperative ^{68}Ga-NEB PET combined with MRL provides advantageous 3-dimensional images, higher temporal resolution, significantly shorter time lapse before image acquisition after tracer injection, more accurate pathological lymphatic vessel distribution than ^{99m}Tc-SC lymphoscintigraphy combined with MRI.

Conclusion—This study documented an effective imaging pattern to combine ^{68}Ga-NEB PET and MRL in patients with lower-limb lymphedema. This strategy demonstrated significant advantage over ^{99m}Tc-SC lymphoscintigraphy/MRL in the evaluation of lymphedema severity, staging and pathological location of lymph vessels to make individualized treatment plan. Dual ^{68}Ga-NEB PET/MRL is thus recommended before the operation for staging and therapy planning.

Keywords

^{68}Ga-NEB; lymphedema; PET-MR; Lymphangiography; Evans Blue Dye; ICG

Introduction

Lower limb lymphedema has become an important medical issue due to its high frequency of occurrence and compromised quality of life, especially in patients who have undergone intra-pelvic or intra-abdominal cancer surgery or radiation treatment [1]. Although conservative nonsurgical treatment has been the dominant therapy for lymphedema, contemporary microsurgical techniques became more popular due to the minor invasiveness and being effective in reducing excess limb volume, the risk of cellulitis, and the need for compression garment use and lymphedema therapy [2–4]. For example, lymphaticovenous anastomosis (LVA) and vascularized lymph node transfer (VLNT) lymphaticolymphatic bypass can treat the excess fluid component of lymphedema swelling that presents as pitting edema [5]. Suction-assisted protein lipectomy (SAPL) is a minimally invasive procedure that addresses the solid component of lymphedema swelling that typically occurs later in the disease process and presents as chronic non-pitting lymphedema [6].

Visualization of the lymphatic system is necessary for identifying and monitoring lymphedema, which is also critical to optimize surgery outcome. However, the localization of the responsible lymph vessels related to lymphedema remains to be a challenge and a time-consuming difficult procedure [7] due to visibility limitations such as diameter of lymph vessels (0.4–0.8 mm) which contains few cells with mainly clear lymph fluid, long-term chronic fibrosis and inflammatory stimulations [8]. To overcome the challenge, various imaging modalities have been applied to assess lymphatic vessels, such as optical imaging by injecting a fluorescent indocyanine green (ICG) dye to provide intraoperative guidance [8–11], magnetic resonance lymphangiography (MRL) [12] and radionuclide lymphoscintigraphy for preoperative evaluation [11, 13–15].

For preoperative imaging, lymphoscintigraphy is a commonly used method by using a scintillation camera to produce repeating 2D images with lymphatic drainage. However, this technique does not allow clear location of lymphatic vessel due to the poor resolution. Besides, ^{99m}Tc-labeled sulfur colloid (SC) are relatively large particles that do not effectively migrate in extremities of patients with lymphedema, resulting in relatively long waiting time before and during scanning. Our previous studies have reported PET lymphangiography with ^{68}Ga-labeled NOTA (1,4,7-triazacyclononane-N,N′,N″-triacetic acid) conjugated truncated Evans blue (NEB), which forms a complex with serum albumin in the interstitial fluid after local injection and allows for rapid visualization of the lymphatic system [16, 17]. Clinical investigations also showed effectiveness of NEB PET in assessing lymph system [18, 19]. On the other hand, MRL has the advantage of higher resolution than gamma scintigraphy or single-photon emission computed tomography (SPECT) lymphoscintigraphy [20, 21]. MRL with contrast enhancement has been used for examining extremity lymphedema, because it can accurately evaluate the anatomical status of lymphatic vessels and lymph nodes in lymphedema [22].

The aim of this prospective study is to evaluate the feasibility of combination of ^{68}Ga-NEB PET lymphangiography with MRL and ICG optical imaging in lymphedema staging and guiding therapy for patients with lower-limb lymphedema.

MATERIALS AND METHODS

Patient recruitment

Patients were recruited from the Therapy Center of Lymphedema Disease in China, Department of Plastic Surgery, Peking Union Medical College Hospital. This clinical study was approved by the Institute Review Board (IRB) of the Peking Union Medical College Hospital and was conducted following the Declarations of Helsinki. All subjects signed written informed consent, and were informed the potential benefits and risks of participating in the investigation. Data were collected in a central database, managed by the Department of Clinical Research of the Peking Union Medical College Hospital, Chinese Academy of Medical Sciences and Peking Union Medical College. This study was registered with ClinicalTrials.gov (NCT02496013).

Enrolled patients were 18 years and older, in suspicion of lymphedema of lower limb, with the history of lymph node dissection and radiotherapy in the groin area. Exclusion criteria consisted of conditions of mental illness, severe liver or kidney disease with serum creatinine >3.0 mg/dl (270 μM) or any hepatic enzyme level 5 times or more than normal upper limit. Participants were also excluded if they were known to have severe allergy or hypersensitivity to IV radiographic contrast, claustrophobia to accept PET or MRI scanning, or female patients in pregnancy or breast feeding.

Clinical staging

According to Common Terminology Criteria for Adverse Events v4.0 (CTCAE), staging was based on the severity of edema limb from foot to groin, degree of skin keratosis or fibrosis (signs and symptoms) [23]. No patient was at stage 0 (or Ia), which refers to a latent

or sub-clinical condition where swelling is not yet evident despite of impaired lymph transport, subtle changes in tissue fluid/composition, and changes in subjective symptoms. 3 patients were diagnosed as stage I, in which pitting edema was found with early accumulation of fluid relatively high in protein content, and subsided with limb elevation. 4 patients were diagnosed as stage II. In these patients, facultative pitting edema was manifest, and limb elevation rarely reduced tissue swelling. 4 patients were diagnosed as stage III without pitting, fat deposits, skin hyperkeratosis, warty overgrowth and elephantiasis.

Imaging Protocols

^{99m}Tc-SC Scintigraphy—All 11 patients received ^{99m}Tc-SC lymphoscintigraphy for comparison within 2 days of ^{68}Ga-NEB PET and MRL. The size of ^{99m}Tc-antimony trisulfide colloidal particles ranged from 16.8 to 23.2 nm. Lymphoscintigraphy acquisition was performed at 1.5 – 6.5 h after the injection of ^{99m}Tc-SC into first and second interdigital spaces of both feet (0.5 mL, 37 MBq/per foot) with a double-head gamma camera with a low-energy high-resolution parallel hole collimator in whole-body scanning mode at a speed of 10 cm/min. More spots and whole body images were obtained for up to 24 h.

^{68}Ga-NEB PET—Preparation of NEB and ^{68}Ga labeling were performed as described in our previous publications [18, 19]. After subcutaneous injection of ^{68}Ga-NEB into the bilateral first web spaces of the feet (0.5 mL, 37 MBq/foot), patients were requested to walk. Thirty minutes later, PET scan was performed from foot to cervical area including thoracic duct (7–9 bed positions, 2 min/bed) after low-dose CT scan (140 kV, 35 mA, pitch of 1:1, 5-mm thickness with 3-mm gap, 512 × 512 matrix, 70 cm field of view) for localization purpose. At 60 and 90 min, PET scans were also performed (5–7 bed positions, 2 min/bed) for each patient, covering from the foot ankle to pubic symphysis (Fig. 1).

MRL

MR lymphangiography was performed with a 3.0 T MR unit (GE Discovery MR 750 3.0T) the day after PET imaging. Unenhanced T_1 and heavily T_2-weighted MRI scans were acquired first and then the contrast agent Gd-DTPA was injected subcutaneously into the bilateral web spaces of the feet (0.6–0.8 mL per injection site). 3D contrast-enhanced MRI images were acquired 2 min later using sequences specialized for lymphatic vessel scans with a slice thickness of 2 mm and a total scan time of 40–50 min (Fig. 1).

Indocyanine Green (ICG) Lymphangiography

All the patients underwent surgical interventions within one week after admission, and have all agreed to receive indocyanine green (ICG) lymphography. 0.1 mL ICG (2.5 mg/mL) was injected sub-dermally between the toes with a 1 mL syringe and a 24 G needle, followed by a foot massage for 5 min from distal to proximal end of the foot. The fluorescence imaging system was developed by the Key Laboratory of Molecular Imaging of Chinese Academy of Sciences [24, 25] (Fig. 1).

Image Analysis

Visual methods were applied for image analysis. Additional comparative reviews were performed between ^{68}Ga-NEB PET, MRL and ^{99m}Tc-SC lymphoscintigraphy. The images were analyzed together by two experienced nuclear medicine physicians, two experienced radiologists together. The criteria of the visual analysis were as followings: (1) Lymphatic vessel visualization of lower extremities (yes/no); (2) The affected lymph vessels line shape; (3) When probe transport/contrast agent transport is identified on PET/MR lymphangiography in each level; (4) Signal intensity on PET/MRL; (5) Dermal backflow(DB) appearance (yes/no); (6) DB area and degree; (7) DB pattern; (8) Thickening and dilated dermal lymphatics (yes/no); (9) Honeycomb Pattern (yes/no); (10) Lymph node accumulation defect degree (high/moderate/low intensity/non-uptake of the PET imaging agent); (11) All imaging analysis criteria above were also based on bilateral comparative analysis; (12) ICG optical imaging (linear/splash/stardust/diffuse).

Imaging guided surgery

Surgical plan was made based on the preoperative imaging information regarding both the function and location of lymph vessels provided by ^{68}Ga-NEB PET and MRL. Patients with stage I lymphedema received multiple lymphaticovenous anastomosis (LVA). Patients with stage II lymphedema received LVA and suction-assisted protein lipectomy (SAPL). Patients with stage III lymphedema received liposuction only. Incisions were made upon the linear pattern lymph vessels identified by ICG and PET-MRL, while the lymphatic vessels and sub-dermal venules were dissected under the fluorescent signal guidance. LVA were performed and proof-checked with ICG fluorescence through the use of surgical navigation system.

RESULTS

Patient demographics

From August 2015 to September 2016, a total of 11 patients (F 9, M 2, age range 29–69 y (49.8 ± 12.4); weight range 51.0–71.0 kg (64.2 ± 7.28)) with different levels of lower limb lymphedema were recruited. These patients had been diagnosed for 1.5–5 years. The diagnosis of lower extremity lymphedema was made by patient’s medical history, physical examination and indirect radionuclide lymphoscintigraphy. Cases with acute inflammation, chronic venous insufficiency, and systemic etiology of edema were excluded from the study.

Preoperative ^{68}Ga-NEB PET and MRL

The lymphatic vessels in the normal lower limbs showed an intermittent, low signal intensity line on MRL and high signal intensity line on ^{68}Ga-NEB PET. The branches could be clearly observed in both images. In contrast, the lymph ducts were viewed as obstructed, beaded, dilated, tissue swollen, and presented with irregularly high signal intensity on PET for the lymphedema affected lower extremities. The affected lymph vessels were also visualized as beaded, dilated, tortuously high signal intensity vessels on MRL with contrast agent infiltrating both dermal and subcutaneous layers.

As functional imaging modalities, both ^{68}Ga-NEB PET and MRL showed different imaging patterns in patients with different lymphedema stages and correlated well with the development of lymphedema. Stage I lymphedema presented less visualized lymphatic vessels, while the delay of probe and contrast agent transport were identified on PET and MR lymphangiography. No obvious dermal backflow appearance of the subcutis was seen at distal abnormal lymph duct, though proximal duct or mild dermal backflow near inguinal region could happen. Lymph node accumulation defect on the affected side with low intensity of the PET tracer was identified compared to the contralateral normal limb (Fig. 2).

Stage II lymphedema presented two types of imaging pattern. Thickening and dilated dermal lymphatics and lymph lakes with sequestered fluid shown as “Honeycomb Pattern” (Fig. 3) were commonly seen in PET and MRL images. Late in stage II, as excess fat and fibrosis supervenes, compensatory vessels could be shown around the damaged lymph vessels with contrast agent accumulation between fat surrounded by fibrotic tissue. Lymph node accumulation defect on the affected side with low intensity to non-uptake of the PET imaging agent was found, with the LNs from contralateral normal limb as reference control (Fig. 3).

In stage III lymphedema, ^{68}Ga-NEB PET and MRL revealed abnormal distribution of contrast agent in the subcutaneous layer as being large, irregular, patchy shaped DB. Increased subcutaneous thickness and diffuse fibrosis were shown in MR imaging, along with locally increased uptake of the PET imaging agent. Both PET and MRL showed dilated lymph vessels and damaged lymph vessels even with severe fibrosis. Tortuous and deep-seated lymph vessels were commonly seen due to overall overgrowth of adipose tissue. Lymph node accumulation defect on the affected side without obvious uptake of the PET imaging agent was observed (Fig. 4).

Differences between ^{68}Ga-NEB PET and ^{99m}Tc-SC lymphoscintigraphy

Compared with ^{99m}Tc-SC lymphoscintigraphy, ^{68}Ga NEB PET/CT images showed better lymphatic channel visualization as early as 30 min after intra-cutaneous injection. The lymphatic channels and veins were also identified clearly in delayed imaging at either 60 or 90 min after tracer injection. In addition, ^{68}Ga-NEB PET lymphangiography showed dermal backflow and lymph node accumulation defect, abnormal lymphatic channels and potential anastomosis pathway. In comparison, the images of ^{99m}Tc-SC lymphoscintigraphy had to be acquired much later (5.5 ± 4.7 h) and repeated delayed imaging to 24 h. ^{99m}Tc-SC lymphoscintigraphy showed dermal backflow and lymph node accumulation defect (Figs. 2–4).

Imaging guided surgery

Based on PET and MRL, we have designed the proper incision sites and performed lymphatico-venous, lymphatico-lymphatic anastomosis and/or liposuction for the lymphedema patients of different stages. The locations of the pathological lymphatic vessels were pinpointed based on the following standard: (i) an intermittent, linear, tubular structure with high signal intensity line on both ^{68}Ga-NEB PET and MRL, and with low signal intensity at the proximal end; (ii) the vessels were found right under dermal and the length

was at least 3 mm. The suitable sized lymphatic channel was prepared for an end-to-end anastomosis and the caliber size was more than 0.3 mm; (iii) no branches or tortuous part; (iv) no contrast agent filtration in surrounding areas.

With the guidance of pre-operative NEB PET and MRL and intraoperative ICG optical imaging, 3 patients diagnosed as stage I lymphedema received multiple lymphaticovenular anastomosis, 4 patients with stage II lymphedema received lymphaticovenular anastomosis and liposuction, and 4 patients with stage III lymphedema received liposuction only. The observations found during surgery were consistent with the findings on PET and MRL images. The surgical interventions went smoothly and no postoperative complications were observed. All patients were discharged within 5 days after surgery.

Discussion

Lymphedema is the result of an overload of lymph fluid that accumulates in the subcutaneous space, causing an increase in limb weight, a decreased limb function, an increased risk of infection, a compromised quality of life, and interference with body appearance [26, 27]. Mapping the lymph system is important in the diagnosis and treatment of lymphedema, especially for surgery interventions [28]. Through ^{68}Ga-NEB PET and MRL, morphologic and functional characteristics of lymphatic vessels in patients with lower extremity lymphedema were visualized. Moreover, the imaging results correlated well with the development of lymphedema. For stage I patients, symptoms are subtle and edema is reversible, thus patients and physicians often ignore the possibility of worsening of lymphatic system. With the disease progression, edema becomes evident, irreversible and in larger scale, but the affected lymphatic vessels have already suffered fibrosis in varying degrees due to long-time inflammation stimulation, which make it difficult for surgeons to ameliorate this situation. For this reason, only liposuction is possible for stage III patients. Therefore, early diagnosis and treatment of lymphedema is important to improve disease prognosis.

Our study confirmed that ^{68}Ga-NEB PET and MRL are synergistic. PET examination could be performed with a large field of view first to locate the range of edema and make assessment of affected lymphatic vessels. MRL could further clarify the degrees of interstitial edema and fibrosis, and point out the position and depth of lymphatic vessels with anatomic accuracy. Thus the combination of both imaging techniques does improve the sensitivity and specificity of early detection of lymphatic lesions. The early abnormal manifestations include delayed radiotracer transport, dermal infiltration and poor visualization of lymphatic collectors, which all suggest the presence of proximal lymphatic flow obstruction.

Surgical interventions for limb lymphedema including LVA and SAPL help reduce the frequency of cellulitis attack and other symptoms [29]. The crucial key to successful LVA is to find the dilated and functional lymphatic vessels to ensure the success of anastomosis [30]. However, it is difficult since the lymph ducts are often sclerotic in the late stage lymphedema [31]. PET/MRL could provide detailed anatomic and functional delineation of the lymphatic system, including the number, caliber, location, and distribution of lymphatic

vessels. This information is very helpful in planning and predicting the lymphatic microsurgery.

The principles of lymphatic imaging using either ^{68}Ga-NEB or ^{99m}Tc-SC are similar. After local injection, ^{68}Ga-NEB complexes with endogenous albumin in the interstitial fluid and allows for visualizing the lymphatic system. For the ^{99m}Tc-SC lymphoscintigraphy, ^{99m}Tc-labeled antimony sulfide colloid move at a rate similar to that of the physiologic flow of lymph and is sufficiently retained by intervening nodes from the interstitial injection site to the lymphatic channels and nodes. However, we found that PET examination is superior to planar whole body ^{99m}Tc-SC lymphoscintigraphy in lymphedema, although both imaging modalities showed dermal backflow and lymph node accumulation defect. With dynamic 3D ^{68}Ga-NEB PET, abnormal lymphatic channels, the location of individual lymphatic channels and potential anastomosis pathway for LVA could be visualized for surgical planning. Continuous bed-positioning facilitates large field of view coverage from feet to cervical area including thoracic duct, which is generally necessary to evaluate lymphatic drainage disorders. Moreover, ^{68}Ga NEB PET lymphangiography takes much less waiting time after contrast injection, and less scanning time for the patients compared with planar whole body ^{99m}Tc-SC lymphoscintigraphy which needs several hours to acquire multiple bed positions or even longer time for repeated delayed planar ^{99m}Tc-SC lymphoscintigraphy imaging.

In clinic, the staging of lymphedema is based mainly on patient history and symptom and still lacks imaging techniques that could provide effective information to assess possible tissue changes related to the stage of lymphedema. ^{68}Ga-NEB PET-MRL showed distinct imaging pattern in different stages of lymphedema, implying that imaging could be useful in staging patient for more precise therapy planning. Indeed, in stage II cases, LVA was performed in the location where the functional lymph vessels could be found in PET/MRL, while liposuction was performed in the fibrosis part of the edema. The imaging strategy significantly reduces the operating time due to its accuracy in locating the lymph vessels prior to surgery. With large field-of-view pre-operative imaging, the severity of lymphedema and the location of abnormal lymphatic vessels can be identified. Intra-operative ICG fluorescence lymphangiography provides focused and direct visualization of those vessels for surgical intervention. We believe both imaging methods are required to guarantee a successful treatment.

Note that the number of study subjects is relative small, but the promising results warrant further large scale clinical trials or expanded clinical applications. In addition, it is very challenging to provide quantitative analysis of the imaging data due to local administration of the imaging agents. The clinical effectiveness depends on careful technical performance and accurate image interpretation. Unfortunately, the conventional lymphoscintigraphy protocol is not standardized and varies according to the diagnostic service.

Conclusion

This study documented an effective imaging pattern to combine ^{68}Ga-NEB PET and MRL in patients with lower-limb lymphedema. This strategy has demonstrated significant advantage in the evaluation of lymphedema severity, staging and pathological location of

lymph vessels to make individualized treatment plan. Dual ^{68}Ga-NEB PET/MR lymphangiography is thus recommended before the operation for lymphedema staging and therapy planning.

Acknowledgments

Author Disclosure Statement

This work was supported by the Intramural Research Program (IRP) of the National Institute of Biomedical Imaging and Bioengineering (NIBIB), National Institutes of Health (NIH); and several research grants to Z. Zhu, which were from National Nature Science Foundation of China (NSFC); Key laboratory of Endocrinology of Ministry of Healthy; and Capital Special Project for Featured Clinical Application. Partial content of this manuscript was presented during the world molecular imaging society 2016 annual meeting in New York, New York.

References

1. Tiwari P, Coriddi M, Salani R, Povoski SP. Breast and gynecologic cancer-related extremity lymphedema: a review of diagnostic modalities and management options. World J Surg Oncol. 2013; 11:237. [PubMed: 24053624]
2. Granzow JW, Soderberg JM, Kaji AH, Dauphine C. Review of current surgical treatments for lymphedema. Ann Surg Oncol. 2014; 21:1195–1201. [PubMed: 24558061]
3. Allen RJ Jr, Cheng MH. Lymphedema surgery: Patient selection and an overview of surgical techniques. J Surg Oncol. 2016; 113:923–931. [PubMed: 26846615]
4. Koshima I, Narushima M, Yamamoto Y, Mihara M, Iida T. Recent advancement on surgical treatments for lymphedema. Ann Vasc Dis. 2012; 5:409–415. [PubMed: 23641262]
5. Sosin M, Yin C, Poysophon P, Patel KM. Understanding the Concepts and Physiologic Principles of Lymphatic Microsurgery. J Reconstr Microsurg. 2016; 32:571–579. [PubMed: 27326801]
6. Granzow JW, Soderberg JM, Dauphine C. A novel two-stage surgical approach to treat chronic lymphedema. Breast J. 2014; 20:420–422. [PubMed: 24943048]
7. Nagase T, Gonda K, Inoue K, et al. Treatment of lymphedema with lymphaticovenular anastomoses. Int J Clin Oncol. 2005; 10:304–310. [PubMed: 16247656]
8. Munn LL, Padera TP. Imaging the lymphatic system. Microvasc Res. 2014; 96:55–63. [PubMed: 24956510]
9. Tiwari A, Cheng KS, Button M, Myint F, Hamilton G. Differential diagnosis, investigation, and current treatment of lower limb lymphedema. Arch Surg. 2003; 138:152–161. [PubMed: 12578410]
10. Vakoc BJ, Lanning RM, Tyrrell JA, et al. Three-dimensional microscopy of the tumor microenvironment in vivo using optical frequency domain imaging. Nat Med. 2009; 15:1219–1223. [PubMed: 19749772]
11. Narushima M, Yamamoto T, Ogata F, Yoshimatsu H, Mihara M, Koshima I. Indocyanine Green Lymphography Findings in Limb Lymphedema. J Reconstr Microsurg. 2016; 32:72–79. [PubMed: 26422172]
12. Neligan PC, Kung TA, Maki JH. MR lymphangiography in the treatment of lymphedema. J Surg Oncol. 2016; doi: 10.1002/jso.24337
13. White RD, Weir-McCall JR, Budak MJ, Waugh SA, Munnoch DA, Sudarshan TA. Contrast-enhanced magnetic resonance lymphography in the assessment of lower limb lymphoedema. Clin Radiol. 2014; 69:e435–444. [PubMed: 25064763]
14. Futamura M, Asano T, Kobayashi K, et al. Prediction of macrometastasis in axillary lymph nodes of patients with invasive breast cancer and the utility of the SUV lymph node/tumor ratio using FDG-PET/CT. World J Surg Oncol. 2015; 13:49. [PubMed: 25885028]
15. Chowdhry M, Rozen WM, Griffiths M. Lymphatic mapping and preoperative imaging in the management of post-mastectomy lymphoedema. Gland Surg. 2016; 5:187–196. [PubMed: 27047786]

16. Zhang W, Wu P, Li F, Tong G, Chen X, Zhu Z. Potential Applications of Using 68Ga-Evans Blue PET/CT in the Evaluation of Lymphatic Disorder: Preliminary Observations. Clin Nucl Med. 2016; 41:302–308. [PubMed: 26859218]
17. Wang Y, Lang L, Huang P, et al. In vivo albumin labeling and lymphatic imaging. Proc Natl Acad Sci U S A. 2015; 112:208–213. [PubMed: 25535368]
18. Zhang J, Lang L, Zhu Z, Li F, Niu G, Chen X. Clinical Translation of an Albumin-Binding PET Radiotracer 68Ga-NEB. J Nucl Med. 2015; 56:1609–1614. [PubMed: 26251416]
19. Niu G, Lang L, Kiesewetter DO, et al. In Vivo Labeling of Serum Albumin for PET. J Nucl Med. 2014; 55:1150–1156. [PubMed: 24842890]
20. Kobayashi H, Kawamoto S, Choyke PL, et al. Comparison of dendrimer-based macromolecular contrast agents for dynamic micro-magnetic resonance lymphangiography. Magn Reson Med. 2003; 50:758–766. [PubMed: 14523962]
21. Niu G, Chen X. Lymphatic imaging: focus on imaging probes. Theranostics. 2015; 5:686–697. [PubMed: 25897334]
22. Arrive L, Derhy S, El Mouhadi S, Monnier-Cholley L, Menu Y, Becker C. Noncontrast Magnetic Resonance Lymphography. J Reconstr Microsurg. 2016; 32:80–86. [PubMed: 25826439]
23. International Society of L. The diagnosis and treatment of peripheral lymphedema: 2013 Consensus Document of the International Society of Lymphology. Lymphology. 2013; 46:1–11. [PubMed: 23930436]
24. Chi C, Du Y, Ye J, et al. Intraoperative imaging-guided cancer surgery: from current fluorescence molecular imaging methods to future multi-modality imaging technology. Theranostics. 2014; 4:1072–1084. [PubMed: 25250092]
25. Chi C, Zhang Q, Mao Y, et al. Increased precision of orthotopic and metastatic breast cancer surgery guided by matrix metalloproteinase-activatable near-infrared fluorescence probes. Sci Rep. 2015; 5:14197. [PubMed: 26395067]
26. Brayton KM, Hirsch AT, PJ OB, Cheville A, Karaca-Mandic P, Rockson SG. Lymphedema prevalence and treatment benefits in cancer: impact of a therapeutic intervention on health outcomes and costs. PLoS One. 2014; 9:e114597. [PubMed: 25470383]
27. Karakousis CP, Driscoll DL, Rose B, Walsh DL. Groin dissection in malignant melanoma. Ann Surg Oncol. 1994; 1:271–277. [PubMed: 7850524]
28. Hidding JT, Viehoff PB, Beurskens CH, van Laarhoven HW, Nijhuis-van der Sanden MW, van der Wees PJ. Measurement Properties of Instruments for Measuring of Lymphedema: Systematic Review. Phys Ther. 2016; 96:1965–1981. [PubMed: 27340195]
29. Sharkey AR, King SW, Ramsden AJ, Furniss D. Do surgical interventions for limb lymphoedema reduce cellulitis attack frequency? Microsurgery. 2016; doi: 10.1002/micr.30115
30. Campisi C, Bellini C, Campisi C, Accogli S, Bonioli E, Boccardo F. Microsurgery for lymphedema: clinical research and long-term results. Microsurgery. 2010; 30:256–260. [PubMed: 20235160]
31. Lohrmann C, Felmerer G, Foeldi E, Bartholoma JP, Langer M. MR lymphangiography for the assessment of the lymphatic system in patients undergoing microsurgical reconstructions of lymphatic vessels. Microvasc Res. 2008; 76:42–45. [PubMed: 18456290]

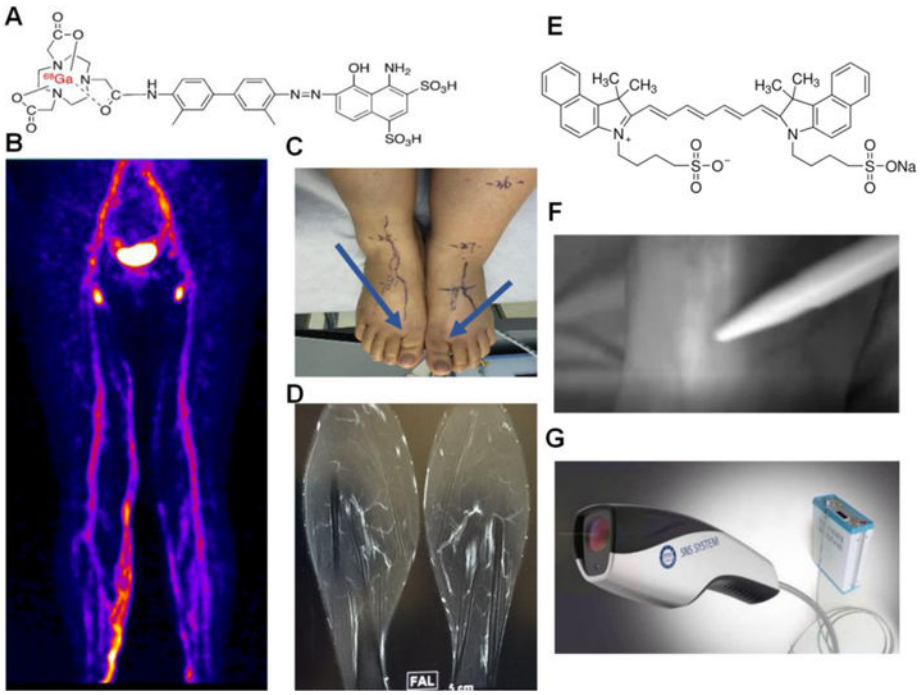

Figure 1.

Imaging procedures of ^{68}Ga-NEB PET/MR/ICG fluorescence lymphangiography. Albumin-binding radiotracer ^{68}Ga-NEB was injected subcutaneously into the bilateral first web spaces of the feet. Patients were requested to walk for 30 min and then PET image acquisition was performed. (A) Structure of ^{68}Ga-NEB. (B) Representative maximum intensity projection of ^{68}Ga-NEB PET with high signal intensity line of the lymphatic vessels acquired at 60 min after tracer administration. (C) Injection site of ^{68}Ga-NEB to a patient with lymphedema. (D) A representative contrast enhanced 3D MR image of lymphatic vessels after subcutaneous injection of Gd-DTPA. (E) Structure of ICG. (F) Real time ICG lymphography acquired intraoperatively. (G) The fluorescence camera used for ICG imaging.

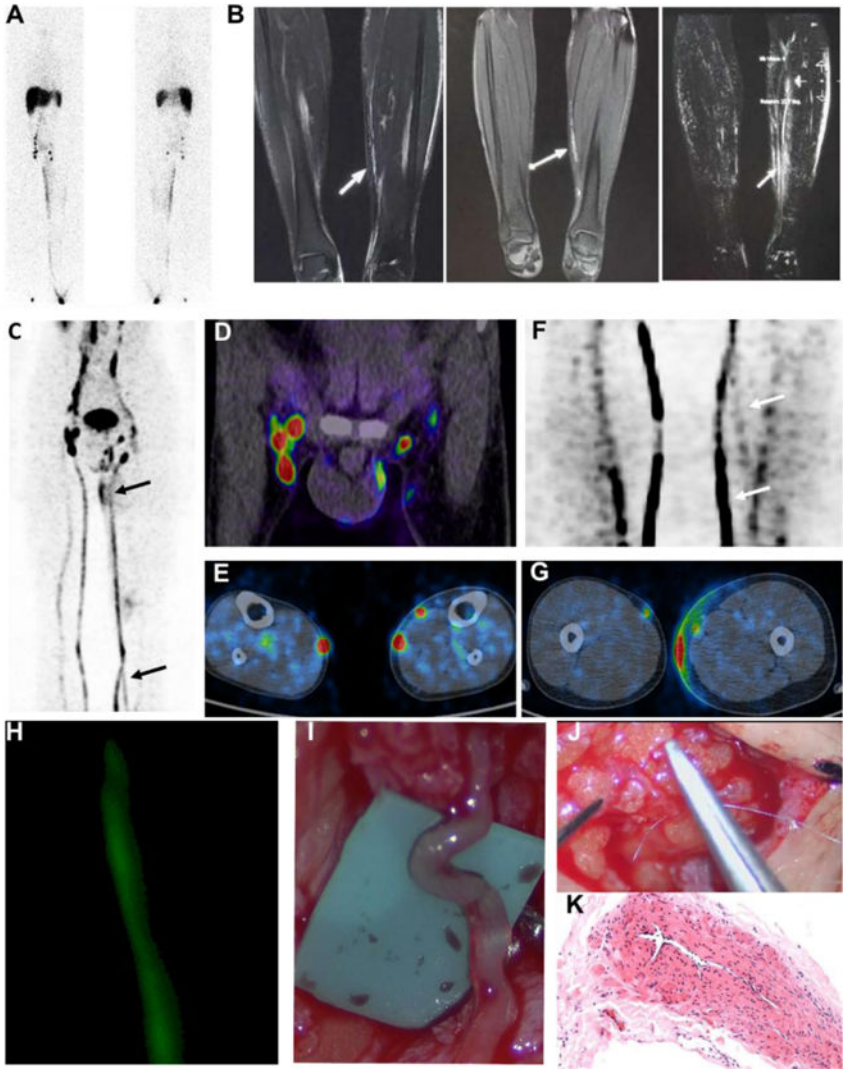

Figure 2.

Imaging guided surgery in a patient with stage I lymphedema. (A) ^{99m}Tc-SC lymphoscintigraphy with anterior and posterior views showed dermal backflow from left calve to thigh and lymph node accumulation defect of the left side. The images were acquired at 6 h after tracer administration; (B) T_1-weighted MR lymphangiography using 3-dimensional gradient recalled echo (LAVA) (left) and fast spin echo (FSE) (middle) showed twisted, compensatory and discontinuous lymphatic channels of left medial calf (arrows). T_1-weighted with LAVA MIP reconstruction (right) showed multi-strip expansion and compensatory channels of left medial calf (arrows). (C–G) ^{68}Ga-NEB PET lymphangiography acquired at 60 min after tracer administration showed slight dermal backflow of the left lower-limb (C and G), lymph node accumulation defect at affected side (C) including left inguinal region (D), abnormal lymphatic channels at left lower medial calve (F) and potential anastomosis pathway inside of medial calf (E). (H) Intraoperative ICG fluorescence lymphangiography provides real-time delineation of subdermal lymphatics inside of medial calf. (I–K) Personalized surgical plan and lymphatic venous anastomosis (LVA) were performed with end-to-end lymphatic channel and suitable sized adjacent

subcutaneous venule anastomosis. A length of dilated channel dissected was further confirmed as the lymphatic vessel (I) with pathological HE staining (K).

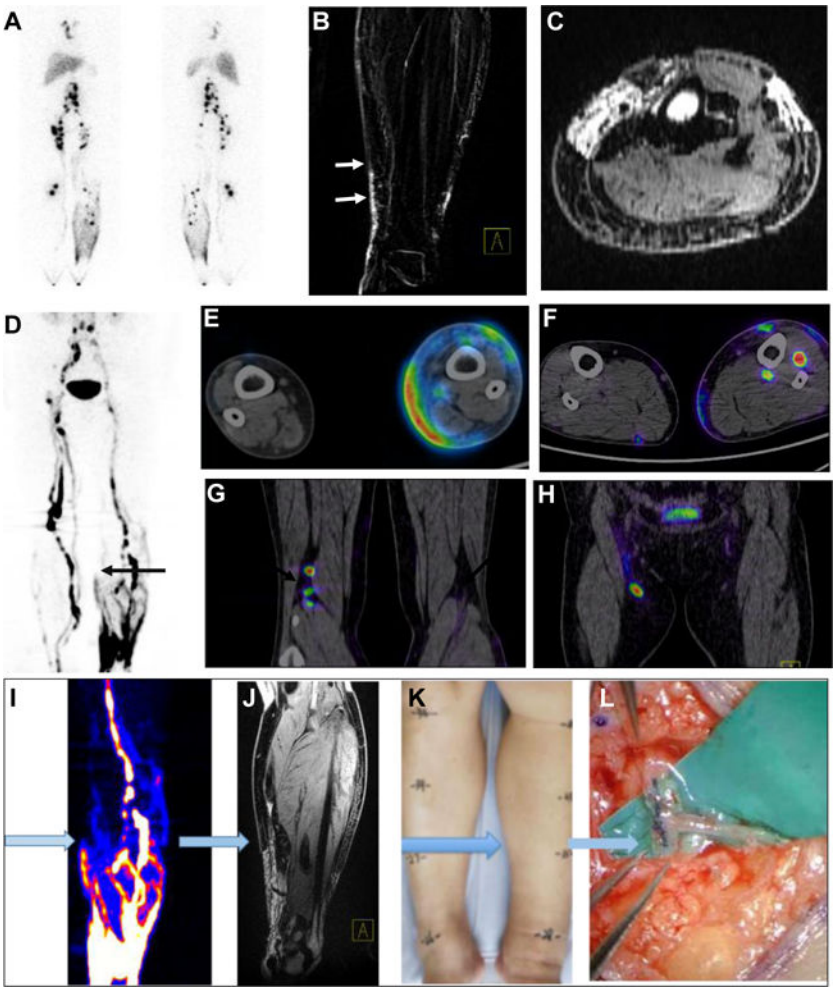

Figure 3.

Imaging guided surgery in a patient with stage II lower-limb lymphedema. (A) ^{99m}Tc-SC lymphoscintigraphy showed dermal backflow of the left lower-limb, asymmetrical distribution of bilateral lymph nodes and accumulation defect on the left side. (B–C) MR lymphangiography showed dilated and discontinuous lymphatic channels of the left medial calf (arrows). (D–H) 68Ga-NEB PET lymphangiography (60 min after tracer administration) represented “Honeycomb Pattern” with dilated dermal lymphatics, discontinuous lymphatic channels and compensatory vessels and lymph lakes of the left lower-limb (D), as well as different levels of dermal backflow (E and F) and lymph node accumulation defect on the affected left side (G and H). (I–L) A typical workflow of imaging guided surgery planning using preoperative ^{68}Ga-NEB PET (I) and MRL (J) to discriminate the location of the lymphatic channels (K) for lymphatic venous anastomosis (L).

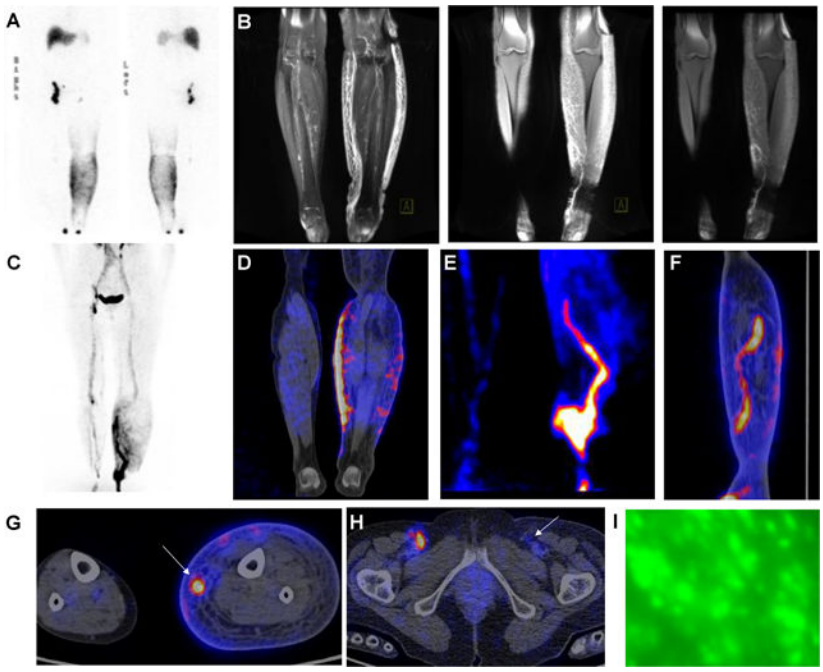

Figure 4.

Imaging guided surgery in a patient with stage III lymphedema. (A) ^{99m}Tc-SC lymphoscintigraphy (6h post injection) showed inguinal lymph node accumulation defect on the left side and dermal backflow of the left lower-limb. (B) MR lymphangiography showed increased subcutaneous thickness and diffuse fibrosis of the left lower-limb, a length of dilated and tortuous deep-seated lymph vessel of the affected medial calve. (C–H) ^{68}Ga-NEB PET lymphangiography (60 min post injection) presented large and diffuse dermal backflow of the lower-limb (C and D), lymph node accumulation defect on the left inguinal region and a length of dilated and tortuous lymphatic channels (E and F) of the affected medial calve. (I) Intraoperative ICG lymphangiography was unable to delineate lymphatic vessels due to limited penetration depth of optical Imaging and overall overgrowth of adipose tissue in stage III lymphedema.

Table 1

Summary of imaging findings and surgical plan in patients with lymphedema

Staging	ICG	PET-CT	MRL	Surgical Plan
Stage I	Linear/Splash	Less visualized lymphatic vessels; delay of probe transport on PET; no obvious DB appearance of the subcutis; lymph node accumulation defect on the affected side	Less visualized lymphatic vessels; delay of contrast agent transport	LVA
Stage II	Stardust	“Honeycomb Pattern”; probe accumulation between fat surrounded by fibrotic tissue; lymph node accumulation defect on the affected side	“Honeycomb Pattern”; contrast agent accumulation between fat surrounded by fibrotic tissue	LVA + SAPL
Stage III	Diffuse	Large, irregular, patchy shaped DB; locally increased tracer uptake; dilated lymph vessels and damaged lymph vessels even with severe fibrosis; tortuous and deep-seated lymph vessels; lymph node accumulation defect on the affected side	Large, irregular, patchy shaped DB; increased subcutaneous thickness and diffuse fibrosis; dilated lymph vessels and damaged lymph vessels even with severe fibrosis; tortuous and deep-seated lymph vessels	SAPL

DB, dermal backflow; LVA, lymphaticovenous anastomosis; SAPL, suction-assisted protein lipectomy